

Light flavor sea-quark asymmetry for the spin-dependent distribution functions of the nucleon¹

M. Wakamatsu[†]

*Department of Physics, Faculty of Science,
Osaka University, Toyonaka, Osaka 560, Japan*

[†] *E-mail: wakamatu@miho.rcnp.osaka-u.ac.jp*

Abstract

The theoretical predictions of the chiral quark soliton model for the unpolarized and longitudinally polarized structure functions of the nucleon are compared with recent high energy data. The theory is shown to explain all the qualitatively noticeable features of the existing experiments, including the light flavor sea-quark asymmetry for the unpolarized distribution functions established by the NMC measurement as well as very small quark spin fraction of the nucleon indicated by the EMC measurement. Another unique feature of the model is that it predicts sizably large isospin asymmetry also for the spin-dependent sea-quark distribution functions.

Key-words: Flavor Asymmetry of Spin Dependent Sea-Quark Distributions, Nucleon Spin Contents, Chiral Soliton, Large N_c QCD

1. Introduction

Undoubtedly, the EMC measurement in 1988 is one of the most surprising discoveries in the recent studies of nucleon structure functions [1]. In my opinion, also very important is the NMC measurement [2], which has established the flavor asymmetry of sea-quark distributions in the nucleon. Why is the 2nd observation so important? Because it is the first clear manifestation of nonperturbative QCD dynamics in high-energy deep-inelastic scattering observables. In fact, the most popular explanation of the NMC measurement is due to the pion cloud effect, which is an inevitable physical consequence of Nambu-Goldstone realization of chiral symmetry.

By now, the NMC observation is known to be explained by several chiral models including the intuitively simplest model, i.e. the Pion Cloud Convolution Model [3] and also the CQSM which we are advocating. However, the physical contents of these two models are not necessarily the same. In fact, we already know that an important advantage of the CQSM over the former is that it is able to explain unexpectedly small quark spin contents of the nucleon simultaneously with the above sea-quark asymmetry [4]. Another important difference will be revealed by considering the following natural question : "Do we expect flavor asymmetric sea also for spin dependent PDF?" As we shall discuss below, the answers of the above two models seem quite different. What makes this difference is an interesting theoretical question, which I shall address in my present talk.

To understand the whole story, it would be helpful to remember some basic features of the CQSM [5],[4] :

¹Invited talk at the XIV International Seminar on High Energy Physics Problems "Relativistic Nuclear Physics and Quantum Chromodynamics", Dubna, 24-29 September, 2000

- First of all, it is a relativistic field theoretical model of baryons effectively incorporating the basic ingredients of large N_C QCD.
- At large N_c , a nucleon is thought to be an aggregate of N_c valence quarks and infinitely many Dirac sea quarks bound by self-consistent pion field of hedgehog shape.
- Canonically quantizing the spontaneous rotational motion of the symmetry breaking mean field configuration, we can perform nonperturbative evaluation of any nucleon observables with full inclusion of valence and Dirac sea quarks.
- Finally, but most importantly, *only 1 parameter* of the model (that is the dynamical quark mass M) was already fixed by low energy phenomenology, so that we can give *parameter-free predictions* for the parton distribution function at the low renormalization scale.

2. CQSM and Twist-2 quark distribution functions

We start with the standard theoretical definition of the quark distribution functions.

$$q(x) = \frac{1}{4\pi} \int_{-\infty}^{\infty} dz^0 e^{ix M_N z^0} \times \langle N(\mathbf{P} = 0) | \psi^\dagger(0) O \psi(z) | N(\mathbf{P} = 0) \rangle |_{z^3 = -z^0, z_\perp = 0}. \quad (1)$$

The following novel N_c dependencies follow from the theoretical structure of the model, i.e. the mean-field approximation and the subsequent perturbative treatment of collective rotational motion [6]–[8] :

$$u(x) + d(x) \sim N_c [O(\Omega^0) + 0] \sim O(N_c^1), \quad (2)$$

$$u(x) - d(x) \sim N_c [0 + O(\Omega^1)] \sim O(N_c^0), \quad (3)$$

$$\Delta u(x) + \Delta d(x) \sim N_c [0 + O(\Omega^1)] \sim O(N_c^0), \quad (4)$$

$$\Delta u(x) - \Delta d(x) \sim N_c [O(\Omega^0) + O(\Omega^1)] \sim O(N_c^1) + O(N_c^0). \quad (5)$$

Notice that, because of the peculiar spin-isospin correlation imbedded in the hedgehog mean field, there is no leading-order N_c contribution to the isovector unpolarized distribution as well as to the isoscalar longitudinally polarized one. This especially means that the isoscalar (or flavor singlet) axial charge is parametrically smaller than the isovector one, in conformity with the EMC observation.

3. Theory versus Experiments

To make a comparison with high energy data, we take the predictions of the CQSM as initial distributions given at low energy scale. Here, we assume that the distribution functions of the s -quark and gluons are both zero at this low energy scale. The scale dependencies of the distribution functions are taken into account by using Fortran code of the standard evolution equation at the NLO [9]. The starting energy of this evolution is fixed to be $Q^2 = 0.30 \text{ GeV}^2$. The model predictions for the twist-2 distribution functions are summarized in Fig.1. In this figure, the long-dashed and dash-dotted curves stand for the contribution of N_c valence quarks and of Dirac-sea quarks, respectively, while

their sums are denoted by solid curves. The functions in the negative x region should be interpreted as antiquark distributions according the rule :

$$u(-x) \pm d(-x) = -[\bar{u}(x) \pm \bar{d}(x)] \quad (0 < x < 1), \quad (6)$$

$$\Delta u(-x) \pm \Delta d(-x) = \Delta \bar{u}(x) \pm \Delta \bar{d}(x) \quad (0 < x < 1). \quad (7)$$

The crucial role of the Dirac-sea contribution is most clearly seen in the isoscalar unpolarized distribution. Here, the “valence-quark-only” approximation leads to positive $u(x) + d(x)$ in the negative x region, thereby violating the positivity of the antiquark distribution [6]. The effect of Dirac-sea quarks is very important also for the isovector unpolarized distribution function. Especially interesting here is the fact that $u(x) - d(x) > 0$ in the negative x region, which means that $\bar{u}(x) - \bar{d}(x) < 0$, in conformity with the NMC observation [8],[10].

Turning to the longitudinally polarized distributions, one observes very different x dependencies between the isoscalar and isovector ones. One interesting feature of the isoscalar distribution is its sign change in the small x region. We shall later see that this sign change is just what is required by the recent deuteron data [11]. Turning to the isovector distribution, we notice that the effect of Dirac-sea quarks has a peak of positive sign around $x \simeq 0$. Noteworthy here is the positivity in the negative x region. It means that sea-quark or anti-quark distribution breaks isospin SU(2) symmetry also for the longitudinally polarized distributions [11].

Given in Fig.2 is a direct comparison with the NMC data for the unpolarized nucleon structure functions. One sees that the difference and the ratio of the proton and neutron structure functions are well reproduced at least qualitatively except for the ratio at the values of x close to 1. Integrating the above difference over x , we obtain $S_G = 0.204$ for the so-called Gottfried sum, which is qualitatively consistent with the NMC analysis, $S_G^{(exp)} = 0.228 \pm 0.007$.

Next, in Fig.3, we compare the predictions for the longitudinally polarized structure functions of the proton, the neutron and the deuteron with the corresponding EMC and SMC data. An excellent feature of the CQSM is a good reproduction of the neutron data, which can also be interpreted as a manifestation of chiral symmetry in high energy observables [8]. Another interesting observation is that the theory closely follows the sign change of the recent deuteron data in the small x region [11]. I emphasize that this sign change of the theoretical structure function can be traced back to the small x behavior of the previously-discussed isoscalar distribution function $\Delta u(x) + \Delta d(x)$.

Now we are in a position to discuss a unique prediction of the model, i.e. the possible isospin asymmetry of the longitudinally polarized sea-quark distribution function. Very little is known for the spin-dependent sea-quark distributions, because inclusive data alone cannot give enough constraint to fix them. Recently, Morii and Yamanishi extracted $\Delta \bar{d}(x) - \Delta \bar{u}(x)$ by using polarized semi-inclusive data, too [12]. Here, the result of their analysis is compared with the prediction of the CQSM [11]. Although the uncertainties of their analysis is too large to draw any decisive conclusion, what is still interesting is their fit given in the following form :

$$\Delta \bar{d}(x) - \Delta \bar{u}(x) = C x^\alpha (\bar{d}(x) - \bar{u}(x)), \quad (8)$$

with

$$C = -3.40, \quad \alpha = 0.567. \quad (9)$$

Here, the negative value of C means that the sign of $\Delta \bar{d} - \Delta \bar{u}$ is opposite to that of $\bar{d} - \bar{u}$, which is just consistent with the theoretical prediction of the CQSM :

$$C \simeq -2.0, \quad \alpha \simeq 0.12. \quad (10)$$

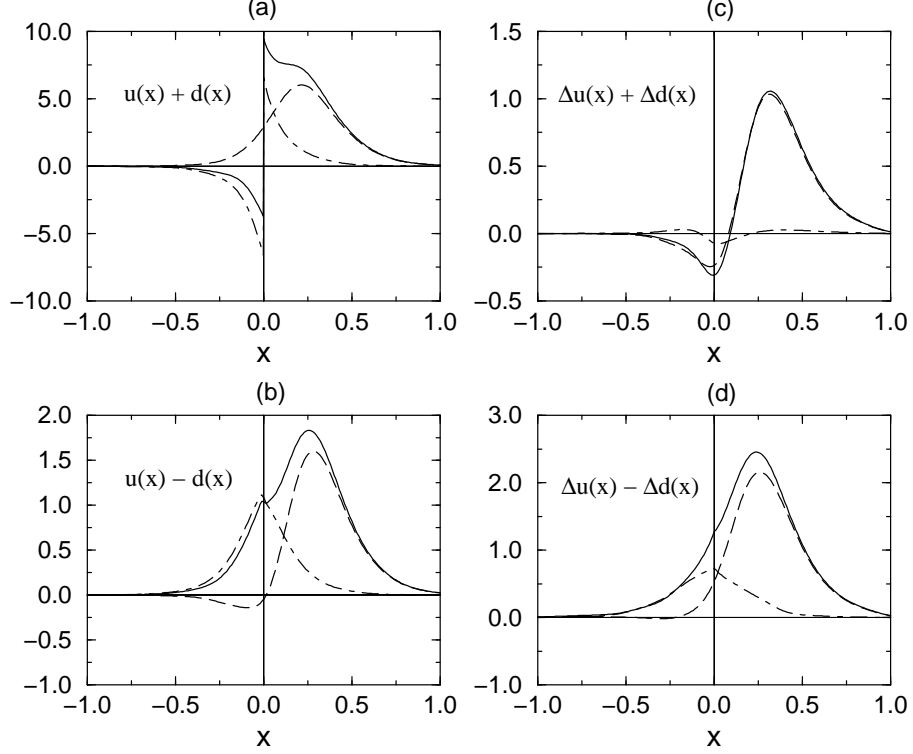


Figure 1: The theoretical predictions of the CQSM for the unpolarized distributions $u(x) + d(x)$ and $u(x) - d(x)$ as well as for the longitudinally polarized distributions $\Delta u(x) + \Delta d(x)$ and $\Delta u(x) - \Delta d(x)$. In all the figures, the long-dashed and dash-dotted curves respectively stand for the contributions of the discrete valence level and that of the Dirac continuum in the self-consistent hedgehog background, whereas their sums are shown by the solid curves.

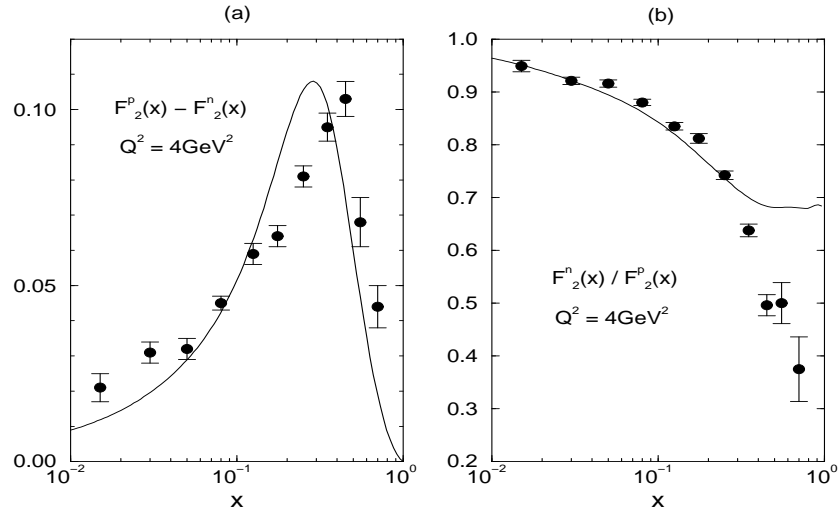


Figure 2: The predictions for $F_2^p(x) - F_2^n(x)$ and $F_2^n(x)/F_2^p(x)$ at $Q^2 = 4 \text{ GeV}^2$ are compared with the NMC data given at the corresponding energy scale.

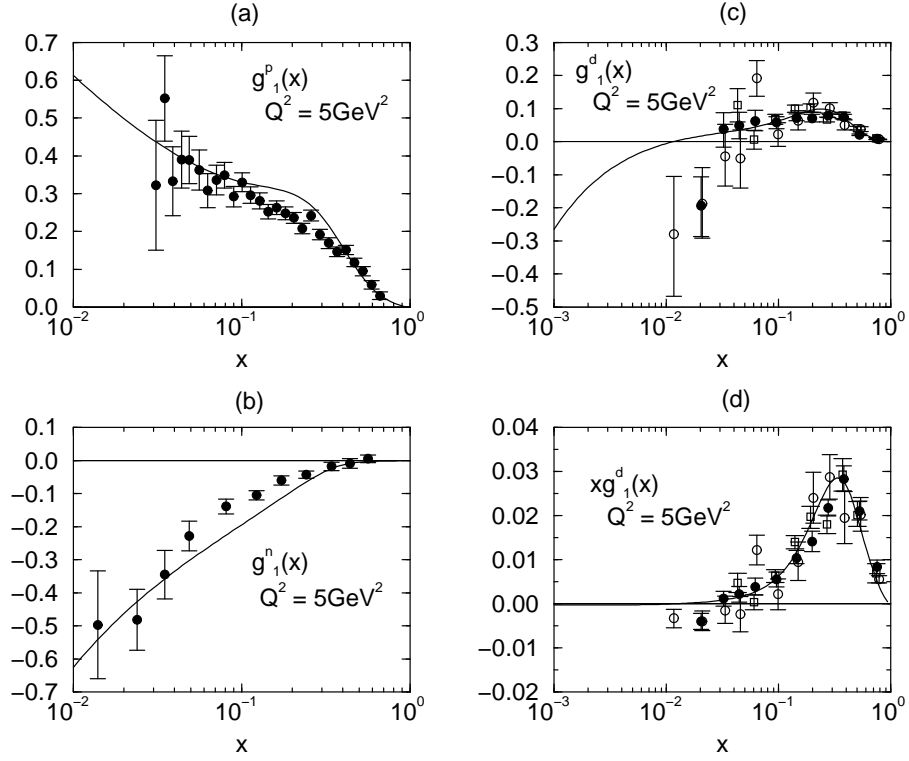


Figure 3: The theoretical predictions for the longitudinally polarized structure functions for the proton, the neutron and the deuteron at $Q^2 = 5 \text{ GeV}^2$ in comparison with the corresponding experimental data. The filled circles in (a) and (b) respectively corresponds to the E143 and the E154 data, whereas the filled circles, the open circles and the open squares in (c) and (d) represent the E143, the E155 and the SMC data.

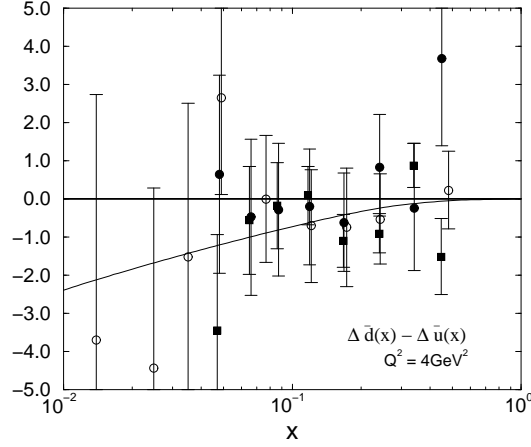


Figure 4: The theoretical predictions for the longitudinally polarized structure functions for the proton, the neutron and the deuteron at $Q^2 = 5 \text{ GeV}^2$ in comparison with the corresponding experimental data. The filled circles in (a) and (b) respectively corresponds to the E143 and the E154 data, whereas the filled circles, the open circles and the open squares in (c) and (d) represent the E143, the E155 and the SMC data.

The fact that C is larger than one is qualitatively consistent with the idea of N_c -counting mentioned before. Undoubtedly, the underlying physics behind this N_c -counting rule is strong spin-isospin correlation imbedded in the hedgehog soliton picture. We emphasize that the Meson Cloud Convolution Model would not predict large spin polarization of sea quarks, since the pion carries no spin and the effect of heavier meson clouds would be much weaker.

Table 1: The separate contributions of quarks and antiquarks to the first moment $\Delta\Sigma$ and L_q at the scale of the model.

| | quark | antiquark | total |
|------------------------|-------|-----------|-------|
| $\Delta\Sigma$ | 0.40 | - 0.05 | 0.35 |
| $2 L_q$ | 0.46 | 0.19 | 0.65 |
| $\Delta\Sigma + 2 L_q$ | 0.86 | 0.15 | 1.00 |

Also very interesting is another consequence of the chiral soliton picture of the nucleon. Shown in Fig.5 are the spin and the orbital angular momentum distribution functions at the model energy scale [13]. One notices that the Dirac-sea contribution to the orbital angular momentum distribution function is sizably large and peaked around $x \simeq 0$. Among others, large support in the negative x region suggests that sizable amount of orbital angular momentum is carried by antiquarks. It can also be confirmed from Table 1 for the corresponding 1st moment [4],[13]. One sees that only 35% of the total nucleon spin comes from quark spin, while the remaining 65% is due to orbital angular momentum of quarks and antiquarks.

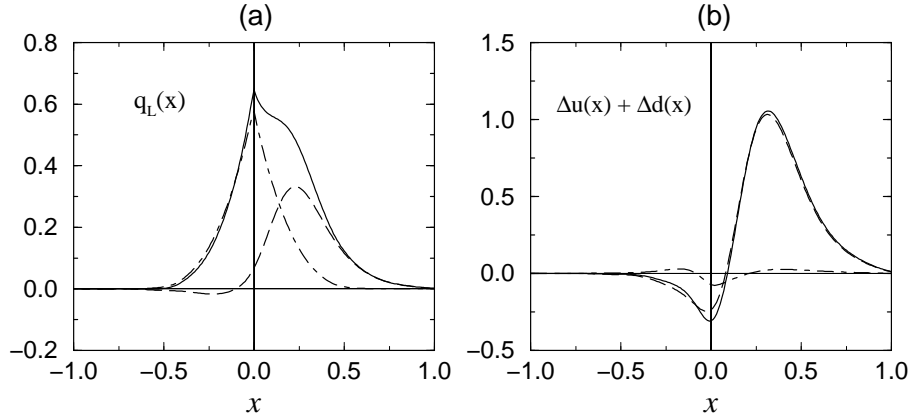


Figure 5: (a) The theoretical predictions of the CQSM for the quark and antiquark orbital angular momentum distribution functions $q_L(x)$ and (b) the isosinglet quark polarization $\Delta u(x) + \Delta d(x)$. The long-dashed and dash-dotted curves respectively stand for the contributions of the discrete valence level and that of the Dirac continuum in the self-consistent hedgehog background, whereas their sums are shown by the solid curves. The distributions with negative x are to be interpreted as the antiquark distributions.

It may be interesting to compare these unique predictions of the CQSM with the recent lattice QCD study of the nucleon spin contents [15]. From the analysis of the energy momentum tensor form factor, they gave an estimate that about 60% of the total nucleon spin is carried by quark field. Further combining this result with the previous estimates of the quark spin content $\langle \Sigma \rangle$, they concluded that, out of this 60%, about 25% comes from intrinsic quark spin, while the remaining 35% is attributed to quark orbital angular momentum. Since the CQSM at the present level of approximation contains no explicit gluon fields, let us tentatively renormalize its prediction by multiplying the above number 60% of the quark angular momentum fraction in the lattice simulation, thereby obtaining the following numbers :

$$\begin{aligned} 60\% \text{ of } \langle \frac{1}{2} \Sigma \rangle^{CQSM} &\simeq 21\%, \\ 60\% \text{ of } \langle L_q \rangle^{CQSM} &\simeq 39\%. \end{aligned}$$

One sees that these numbers are rather close to the corresponding numbers 25% and 35% in the lattice QCD. At least, one can confirm an interesting common feature, i.e. the dominance of the orbital angular momentum part over the intrinsic spin one.

Although qualitatively interesting, one should not put too much confidence on the precise numbers obtained in the lattice QCD calculation at the present stage. To illustrate it, we compare in Fig.6 its predictions for the twist-3 matrix element of $g_2(x)$ with those of other models including the CQSM [14]. To be more precise, what is compared here is the third moment of the twist-3 part of the spin structure function $g_2(x)$.

$$d_2(Q^2) \equiv 3 \int_0^1 x^2 \bar{g}_2(x, Q^2) dx = 2 \int_0^1 x^2 \left[g_1(x, Q^2) + \frac{3}{2} g_2(x, Q^2) \right] dx. \quad (11)$$

The lattice QCD as well as the QCD sum rule fail to reproduce d_2 of the proton and neutron at the same time, while the CQSM as well as the MIT bag model give relatively good reproduction of the E155 data [22].

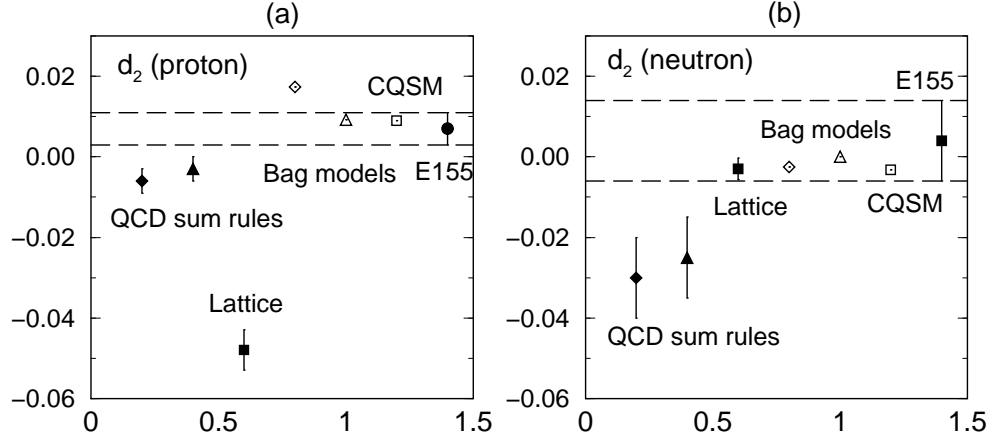


Figure 6: The predictions of various theoretical models for the twist-3 matrix element d_2 for the proton and the neutron are compared with the recent E155 analysis [22]. Shown theoretical models are from left to right : QCD sum rules [16],[17], lattice QCD [18], MIT bag models [19],[20], and the CQSM [14].

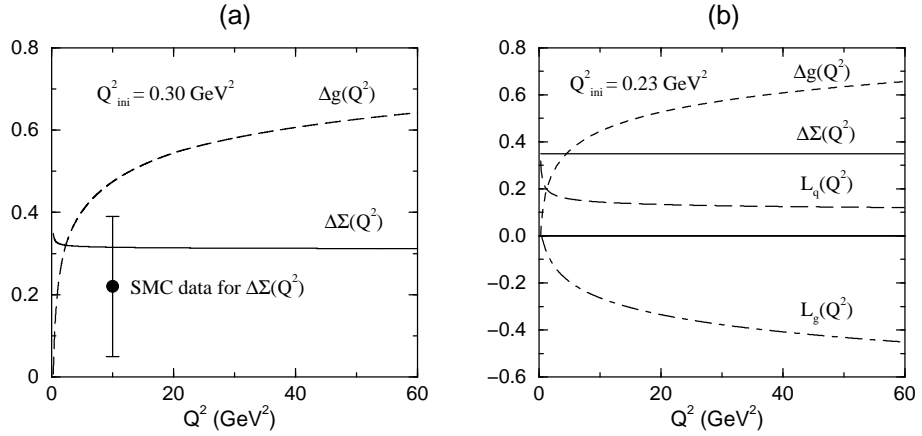


Figure 7: (a) NLO evolution of $\Delta\Sigma(Q^2), \Delta g(Q^2)$ (b) LO evolution of full nucleon spin contents

The spin and orbital angular momentum contents of the nucleon are of course scale-dependent quantities. Here, Fig.7(a) shows the scale dependence of the quark and gluon longitudinal polarization at the NLO, while Fig.7(b) does the scale dependence of the full nucleon spin contents including the orbital angular momentum but at the LO [13]. The initial energy scale of the LO evolution equation is chosen to be a little smaller than the NLO case, so that both give a similar Q^2 -evolution for Δg . At the NLO with \overline{MS} scheme, $\Delta\Sigma$ is known to have weak scale dependence mainly at low Q^2 . The theoretical value $\Delta\Sigma = 0.31$ obtained at $Q^2 = 10 \text{ GeV}$ is qualitatively consistent with the result of the recent SMC analysis $\Delta\Sigma_{SMC}^{(exp)} = 0.22 \pm 0.17$ [23]. Another remarkable feature is that the gluon polarization Δg grows rapidly as Q^2 increases, even if we assume zero polarization at the low renormalization point.

4. Conclusion

To sum up, I have shown that, *without introducing any adjustable parameter* except for the initial-energy scale of the Q^2 -evolution, the CQSM can explain all the qualitatively noticeable features of the recent high-energy deep-inelastic scattering observables. It naturally explains the excess of \bar{d} -sea over the \bar{u} -sea in the proton. It also reproduces qualitative behavior of the observed longitudinally polarized structure functions for the proton, neutron and the deuteron. The most puzzling observation, i.e. unexpectedly small quark spin fraction of the nucleon can also be explained in no need of large gluon polarization at the low renormalization point. Finally, as a unique prediction of the model, I pointed out the possibility of large isospin asymmetry of the spin-dependent sea quark distributions, which has also been suggested by the recent semi-phenomenological analysis of Morii and Yamanishi. I emphasized that the obtained result $|C| > 1$ in the parametrization $\Delta\bar{d}(x) - \Delta\bar{u}(x) = C x^\alpha (\bar{d}(x) - \bar{u}(x))$ is a natural consequence of the N_c -counting rule, but it appears inconsistent with the naive Meson Cloud Convolution Model. Then, if this large asymmetry of the longitudinally polarized sea is experimentally established, it would offer a strong evidence in favor of nontrivial spin-isospin correlation imbedded in the “large N_c chiral soliton picture” of the nucleon.

The talk is based on the collaborations with T. Watabe and T. Kubota.

References

- [1] EMC Collaboration, J. Ashman et al., Phys. Lett. **B206** (1988) 364-370 ; Nucl. Phys. **B328** (1989) 1-35.
- [2] NMC Collaboration, P. Amaudruz et al., Phys. Rev. Lett. **66**, 2712 (1991).
- [3] See, for instance, S. Kumano, Phys. Rep. **303** (1998) 183.
- [4] M. Wakamatsu and H. Yoshiki, Nucl. Phys. **A524** (1991) 561.
- [5] D.I. Diakonov, V.Yu. Petrov, and P.V. Pobylitsa, Nucl. Phys. **B306** (1988) 809.
- [6] D.I. Diakonov, V.Yu. Petrov, P.V. Pobylitsa, M.V. Polyakov, and C. Weiss, Nucl. Phys. **B480** (1996) 341; *ibid.*, Phys. Rev. **D56** (1997) 4069.
- [7] M. Wakamatsu and T. Kubota, Phys. Rev. **D57** (1998) 5755.
- [8] M. Wakamatsu and T. Kubota, Phys. Rev. **D60** (1999) 034020.

- [9] M. Hirai, S. Kumano, and M. Miyama, Compt. Phys. Commun. **108** (1998) 38; *ibid.*, **111** (1998) 150.
- [10] P.V. Pobylitsa, M.V. Polyakov, K. Goeke, T. Watabe and C. Weiss, Phys. Rev. **D59** (1999) 034024.
- [11] M. Wakamatsu and T. Watabe, Phys. Rev. **D62** (2000) 017506.
- [12] T. Morii and T. Yamanishi, Phys. Rev. **D61** (2000)
- [13] M. Wakamatsu and T. Watabe, Phys. Rev. **D62** (2000) 054009.
- [14] M. Wakamatsu, Phys. Lett. **B487** (2000) 118.
- [15] N. Mathur, S.J. Dong, K.F. Liu, L. Mankiewics, and N.C. Mukhopadhyay, hep-ph / 9912289.
- [16] E. Stein, Phys. Lett. B343 (1995) 369.
- [17] I. Balitsky, V. Braun and A. Klesnichenko, Phys. Lett. B242 (1990) 245 ; B318 (1993) 648(E).
- [18] M. Göckeler et al., Phys. Rev. D53 (1996) 2317.
- [19] X. Ji and P. Unrau, Phys. Lett. B333 (1994) 228.
- [20] F.M. Steffens, H. Hoffmann and A.W. Thomas, Phys. Lett. B358 (1995) 139.
- [21] X. Song, Phys. Rev. D54 (1996) 1955.
- [22] E155 Collaboration, P.L. Anthony et al., Phys. Lett. B458 (1999) 529.
- [23] SMC Collaboration, B. Adeva et al., Phys. Rev. **D58** (1998) 112001.